Available online at www.sciencedirect.com
ScienceDirect
Sensors and Actuators A 135 (2007) 236–243
SENSORS AND ACTUATORS A PHYSICAL
www.elsevier.com/locate/sna

Polymer magnetic scanners for bar code applications

Arda D. Yalcinkaya [a,*], Olgaç Ergeneman [b], Hakan Urey [b]

[a] *Bogazici University, Electrical and Electronics Engineering Department, College of Engineering, TR 34342 Bebek, Istanbul, Turkey*
[b] *Koç University, Electrical and Electronics Engineering Department, College of Engineering, Rumelifeneri Yolu, TR 34450 Sariyer, Istanbul, Turkey*

Received 20 February 2006; received in revised form 2 June 2006; accepted 15 June 2006
Available online 22 August 2006

Abstract

Resonant mode polymer-based electromagnetic scanners are developed for barcode reading applications. The electromagnetic scanner consists of a mirror suspended by a polymer cantilever beam, a permalloy sheet attached to the mirror, and an external coil to generate the driving magnetic field. The simple fabrication process involves polymer molding and electroplating of magnetic material, yielding inexpensive devices suitable for high volume manufacturing.

Mechanical and magnetic modeling of the device as well as analytical, numerical and experimental results are presented. A barcode reading system is demonstrated successfully using this inexpensive, easy to manufacture scanner. Fabricated cantilever scanners achieve an optical $\theta{\cdot}D$ product of 123° mm at 56.5 Hz, consuming an actuation power of 168 mW. 2D actuation of the cantilever scanners is also demonstrated.

Keywords: Electromagnetic actuation; Optical scanners; Polymers; Permalloy; Barcode readers

1. Introduction

Performance of a barcode reading system is dependent on the properties of the barcode, such as minimum bar width, contrast, code length, code height and barcode quality as well as the scanner used in the system. Scanning mirrors, holographic scanners, and rotating prisms are commonly used optical components in barcode readers to form a scan line on a sequence of dark bars on a light background. Regardless of its type, in such a barcode reading system, coding information is contained in the relative widths or spacings of the dark bars and light spaces. Polygon scanners have been widely used in the bar code reading applications, but this type of scanners suffer from relatively high power consumption, bulky size and the necessity of a motor to drive the polygonal scan mirror [1].

The presented device is not limited to barcode reading applications and can also be used for general scanned imaging applications. Development of polymer scanners for barcode reading applications is driven by the need for an inexpensive, compact, low resonant frequency scanner suitable for volume manufacturing. Combination of electromagnetic actuation technique with polymer scanners is especially useful to obtain large mirror rotation angles to produce wide scan lines at low power levels. Specification on scan line width is normally translated into scan mirror performance by $\theta_{opt}D$ product, where D is the rotating mirror size and θ_{opt} is the optical scan angle (which is equivalent to twice the mechanical rotation angle). Typical barcode reading applications require $\theta_{opt}D$ to exceed $\pm 10^{\circ}$ mm [1]. An electromagnet and a polymer scanner with magnetic material can be utilized to achieve a system with the desired properties. In addition to this, silicon-based MEMS microscanner fabrication involves expensive process steps such as photo mask fabrication, lithography, etching. Silicon MEMS microactuators for other applications are presented in a number of references [3–8] are mostly meant for resonance frequencies that demand expensive read out electronics. Moreover, relatively large silicon die area adds up to the product cost. Previously reported MEMS-based electrostatic scanners for barcode readers [14,16] require high dc polarization voltages (~30 V) for the operation, limiting the use in the portable systems. In contrast to conventional Si micromachining, larger material volume used for polymers help to lower the production costs and allow utilization of cheap processes such as mould shaping and UV curing. Furthermore, low resonant frequency scanners made of polymers allow headroom for signal processing electronics in terms of speed and power consumption. Recently, barcode scanners based on high-speed

* Corresponding author. Tel.: +90 212 338 1709; fax: +90 212 338 1548.
E-mail address: arda.yalcinkaya@boun.edu.tr (A.D. Yalcinkaya).

0924-4247/$ – see front matter © 2006 Elsevier B.V. All rights reserved.
doi:10.1016/j.sna.2006.06.059

infrared tunable laser integrated with a diffraction grating is proposed for 1D barcode reading [13], however this method suffers from the high cost of the components used in the system as well as the limited scan angle.

In this paper, electromagnetically actuated polymer-based scanning mirrors are presented. A brief overview of the scanner design and the analytical modeling of the mechanical part are given in Section 2.1. Electromagnetic actuation scheme is explained in Section 2.2, where finite element analysis (FEA) of structural mechanics and electromagnetic forces are supplied. Experimental work and characterization results of the devices are outlined in Section 3. Section 4 describes the fabrication of the devices. Application to barcode reading and also 2D image scanning are presented in Section 5 and finally, conclusions are supplied in Section 6.

2. Actuator design

2.1. Structure of the scanners

Schematics of scanners studied in this paper is shown in Fig. 1(a). This cantilever type scanner is based on a mirror with a size of $W_2 \times L_2$ attached to a L_1 long W_1 wide suspension anchored at the end to a larger frame. The uniform thickness of the polymer is t_1 and selective deposition of t_2 thick nickel–iron permalloy is performed beneath the mirror. In order to have a flat mirror with surface deformations less than one-tenth of the wavelength used in the system, an Al coated Si mirror diced into

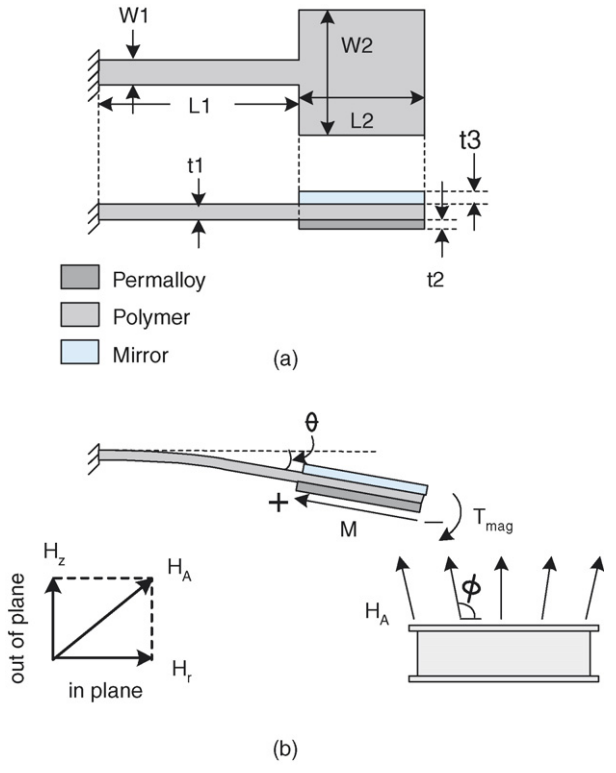

Fig. 1. Scanner mechanical schematics and dimensions.

Table 1
Parameter definition and values for cantilever type scanner

Parameter	Symbol	Cantilever
Width of the suspension	W_1	1 mm
Width of the mirror	W_2	8 mm
Length of the suspension	L_1	15 mm
Length of the mirror	L_2	8 mm
Structure thickness	t_1	0.5 mm
Permalloy thickness	t_2	30 μm
Si die thickness	t_3	0.5 mm

desired size with a thickness of t_3 is attached to the front side (Table 1).

Cantilever type scanner is designated to have its fundamental resonance mode in the out-of-plane direction. Excitation of this mode is performed by creating an alternating force component normal to the surface of the scan mirror. Light beam falling onto the scan mirror is deflected by the scanner to form a scan line on a desired target. The first resonance mode frequency (ω_0) of the cantilever type scanner is calculated as:

$$\omega_0 = \sqrt{\frac{k_s}{J_{eff}}} \tag{1}$$

where k_s is the stiffness of the suspension calculated through the Young's modulus of the polymer and the geometry of the spring. J_{eff} is the effective mass moment inertia. Essentially, one can tailor the resonance frequency by changing the size of the scanner. Finite element modeling is used in simulation of the mode frequencies and shapes for validating the analytical calculations. Fig. 2 shows the first four mode shapes of the polymer cantilever structure, where the mirror and the magnetic plating is not included to the FEA model. The fundamental mode is used for 1D scan operation for barcode readers, where the scanning mirror is moving out-of-plane at 79 Hz. Note that this FEM analysis is performed using only the polymer structure, as will be explained in Section 3, the actual resonance frequency will be smaller that 79 Hz due to the extra weight coming from the silicon mirror die and the magnetic material. The second mode is an in-plane bending mode, which occurs at 387 Hz. The third mode is the torsion about the suspension and is utilized to form a scan line orthogonal to the one created by the fundamental mode for 2D scanning. Finally, the fourth mode is the second order bending mode of the cantilever where most of the deformation happens in the suspension at 746 Hz. It is worth noticing that the scanner works as a coupled multi band-pass filter, where modes are well separated due to the moderately high quality factor of each mode.

2.2. Electromagnetic actuation force

An electromagnet is placed under the magnetic material to generate the driving magnetic field, H_A, as shown in Fig. 1(b). The deflection of the scanner is modeled using the balance between the magnetic torque T_{mag} and the mechanical restoring torque T_{mech}. For thin film soft magnetic materials the easy axis remains in the film-plane due to strong shape anisotropy.

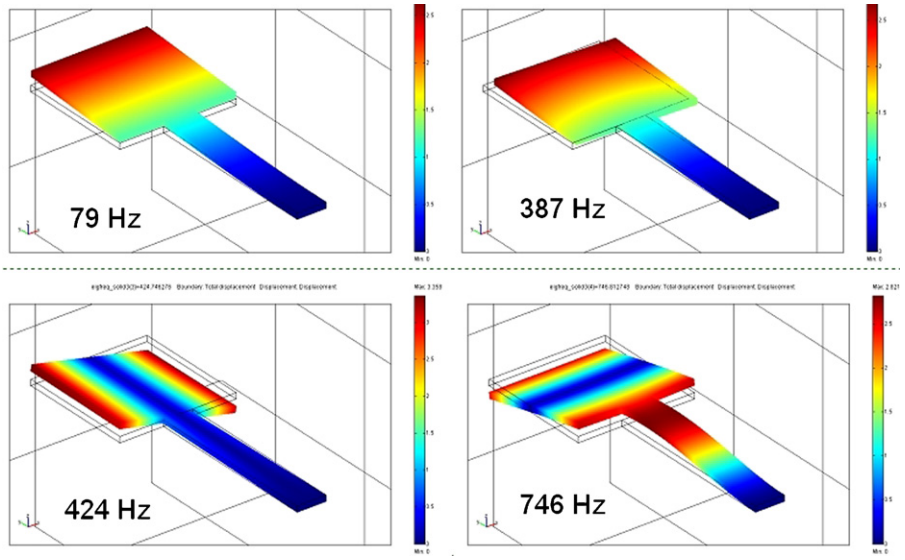

Fig. 2. FEM structural analysis results showing the mode shapes of the cantilever type scanner: (1) out-of-plane bending mode; (2) in-plane bending mode; (3) torsion mode about the spring; (4) structural rocking mode. In this simulation only polymer-based structural material is analyzed.

The magnetostatic torque can be expressed as [2,4,8]:

$$T_{\text{mag}} = VM_{\text{p}}H_{\text{A}}\sin(\phi - \theta) \tag{2}$$

where $V = W_2L_2t_2$ is the magnet volume, M_{p} the magnetization of the permalloy induced by the external field H_{A}, θ the scan angle, and $(\theta - \phi)$ is the angle between H_{A} and M_{p} Note that θ, H_{A} and M_{p} changes with time as the scanner moves. Eq. (2) assumes ϕ and H_{A} are not varying with position across the scanner. The deflection angle of the scanner for small deflections is given by [9]:

$$\theta = -\frac{T_{\text{mech}}}{k_{\text{s}}} \tag{3}$$

The stiffness of the mirror piece is much greater than the stiffness of the suspension beam, therefore the bending of the mirror is negligible and is not considered in this paper. Likewise, the moment of inertia of the cantilever is small compared to the one of silicon mirror and therefore it is neglected. Both of these assumptions are verified with FEM simulations.

Large static deflection of permalloy actuators has been studied in a number of papers [4,6]. This work focuses on the permalloy actuator's small angle rotations and its dynamic actuation characteristics. The magnetization of the permalloy sheet is assumed to remain along the easy axis which is parallel to the surface caused by the high magnetic shape-anisotropy [4]. For thin films, when an external field is applied, the magnetization vector remains parallel to the film plane and a mechanical torque is produced to align the magnetic film with the external magnetic field lines.

The magnetic field simulations for small excitation signals are performed using finite element modeling software (FEMLAB) [10]. In the simulation test bench, a large coil with 68 mm outer diameter and 60 mm length incorporating a 16 mm diameter magnetic core at its center is defined. Coil geometry used in this work is sketched in Fig. 3(a). Finite element analysis of magnetic flux lines for this specific coil is performed and the results are shown in Fig. 3(b). Both radial and out-of-plane components of the magnetic field created by the coil is simulated as a function of the distance to the coil. The radial component

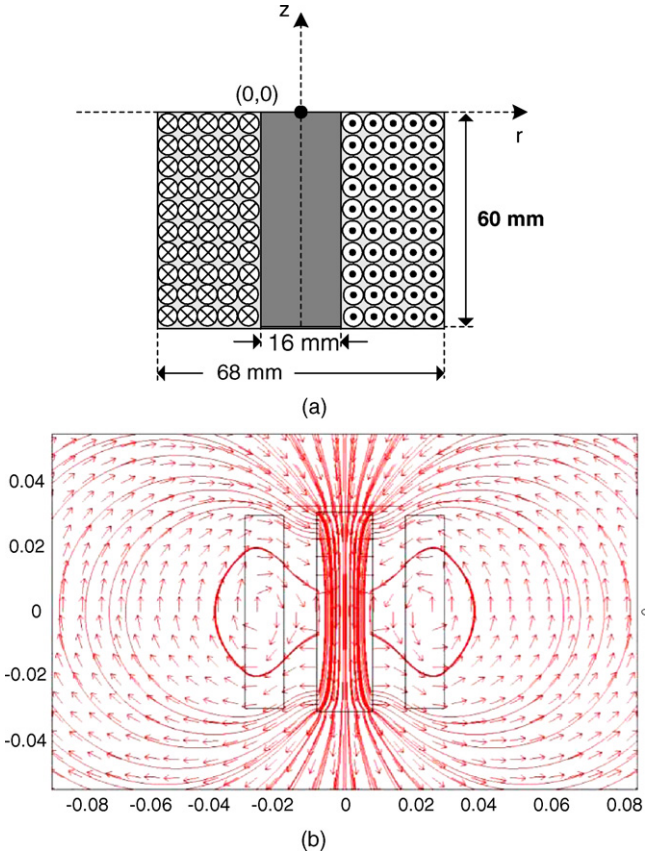

Fig. 3. (a) Coil geometry used in this work; (b) cross section of the coil with the magnetic core. Magnetic field and magnetic flux density generated by the described coil. The arrows show the magnetic flux density and the streamline shows the magnetic field.

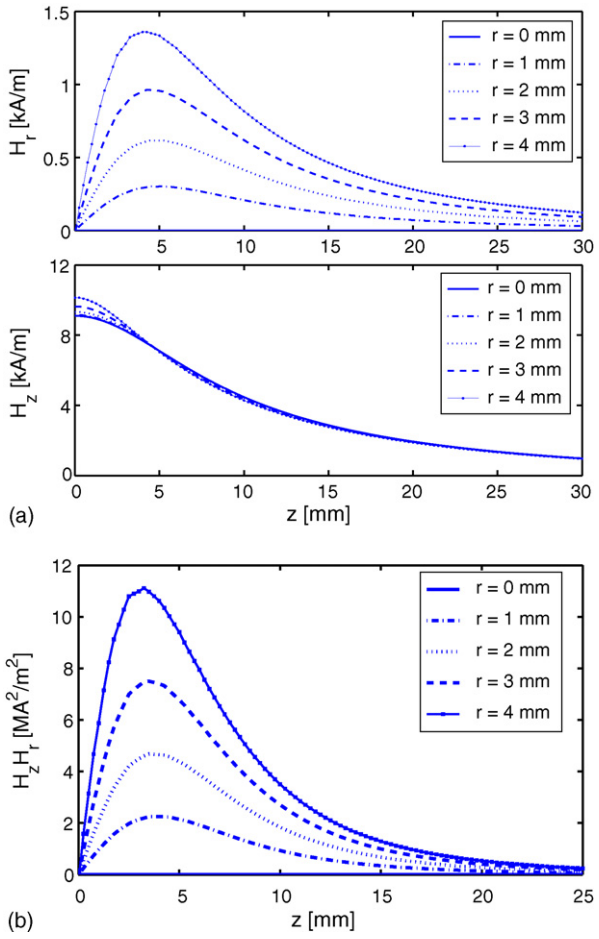

Fig. 4. FEM simulations of: (a) the in-plane, H_r, and out-of-plane, H_z component of the magnetic field H_A; (b) the product of H_r and H_z plotted vs. distance between the coil and permalloy sheet taken at different radial distances from the central axis.

magnetizes the sample and the vertical component generates the torque on this magnetization.

Fig. 4(a) shows the in-plane (H_r) and out-of-plane (H_z) components of the magnetic field versus the distance between the coil and the permalloy sheet. As can be seen from this plot, the maximum radial field is obtained at about 3.5 mm away from the electro coil. For small drive currents, the magnetic material is not saturated and M_p is proportional to H_r. Thus, $M_p \times H_r$ product, illustrated in Fig. 4(b), can be taken as proportional to the magnetic torque.

According to Fig. 4(b), the maximum actuation torque can be achieved by placing the permalloy sheet about 3.5 mm from the the coil defined in Fig. 3(a). In order to verify FEA simulations, the experimental peak-to-peak deflection of the scanner is extracted by placing the device at the center of the coil. The device is actuated by a small sinusoidal current waveform with an offset at the scanner's resonant frequency. Scanner tip deflection as a function of the distance between the coil and permalloy is given in Fig. 5, which clearly demonstrates that the displacement of the cantilever tip, thus the magnetic actuation force is maximum around 3.5 mm. The product of $H_r \times H_z$ increases as we depart from the central axis.

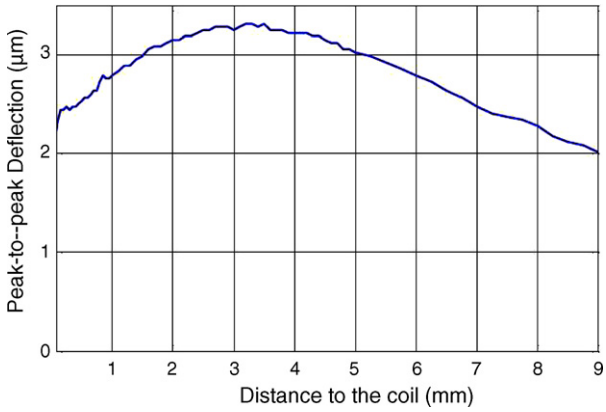

Fig. 5. Peak-to-peak deflection of the scanner vs. the distance between the coil and the permalloy sheet measured for small drive currents at $r=0$ (i.e., the scanner is centered on top of the coil).

3. Experimental results

The dynamic deflection of the scanner was measured using a laser doppler vibrometer (LDV) by using the setup illustrated in Fig. 6. This setup allows characterization of electromechanical transfer function of the device, yielding gain–phase plots. Fig. 7(a) shows the peak-to-peak deflection of the cantilever tip as a function of frequency when drive currents varying between 2 mA and 16 mA are applied to the electro coil. As the drive current, thus the magnetic field, is increased, a slight reduction in the resonance frequency is observed, due to the spring softening effect at large displacements. The minimum $\theta_{opt}D$ of $\pm 10^\circ$ mm, adequate for bar code scanning application, is obtained at a power level of 2 mW. Experiments have shown that the peak-to-peak optical $\theta_{opt}D$ product of 123° mm (15.8° of optical scan angle using a 8 mm mirror) can be obtained with a power consumption 168 mW. Fig. 7(b) shows the peak scan angles of the tip displacements for different drive currents. The mechanical transfer fuction showing the out-of-plane bending and the torsional modes of the device is given Fig. 7(c). In order to obtain this experimental data, the LDV spot is shined onto the corner of the scanner mirror (as shown in the inset of Fig. 7(c)), where both

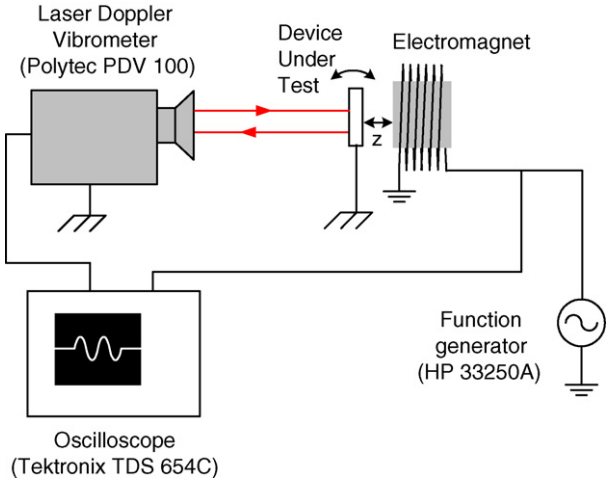

Fig. 6. The setup used for electromechanical transfer function characterization.

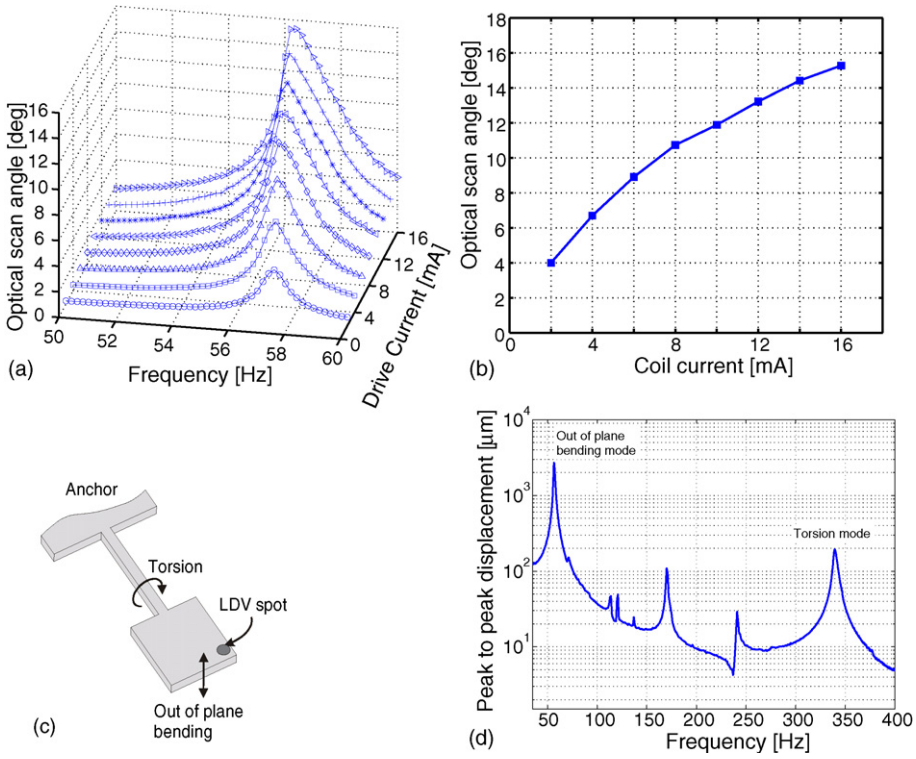

Fig. 7. Mechanical characterization of the scanner performed in ambient air: (a) resonance peaks of the scanner for different electro coil currents; (b) cantilever tip displacement at out-of-plane bending mode resonance for varying actuation currents; (c) schematic showing the point where the LDV measurements are taken; (d) mechanical transfer function of the device, showing the mirror corner displacement as a function of frequency between 40 Hz and 400 Hz.

out-of-plane bending motion and torsion of the scanner are easily detected. The modes associated with the out-of-plane bending and the torsion of the scanner occurs at 56.5 Hz and 340 Hz, respectively. The mechanical quality factors of these motions, measured at atmospheric pressure, are 40 (out-of-plane mode) and 87 (torsion mode). Frequency spectrum of the device in a window between 40 Hz and 400 Hz is given Fig. 7(d). In addition to the aforementioned out-of-plane bending mode and torsion mode, there are two more mode peaks appearing at 170 Hz which is due to the subharmonic excitation of the torsion mode and 240 Hz due to out-of-plane rocking motion.

An interesting, yet useful property of the present device is its ability to produce two dimensional scan patterns, as shown in Fig. 8. This 2D image is created by using only one actuation coil and driving the scanner with a signal given as:

$$i_d = I_1 \sin \omega_1 t + I_2 \sin \omega_3 t \quad (4)$$

where ω_1 and ω_3 are the resonance frequencies of the out-of-plane bending and torsion modes of the scanner, and I_1 and I_2 are the magnitudes of the currents exciting the corresponding modes, respectively. In effect, by applying a drive current given in Eq. (4), the scanner is kept in two-mode coupled resonance where each resonance mode yields in a scan line orthogonal to the other one. Moderately high mechanical quality factors of the modes separate the motions in two axes, acting as a band-pass filter with multi pass bands. A similar actuation principle was previously applied to Lorentz force electromagnetic MEMS scanners [12].

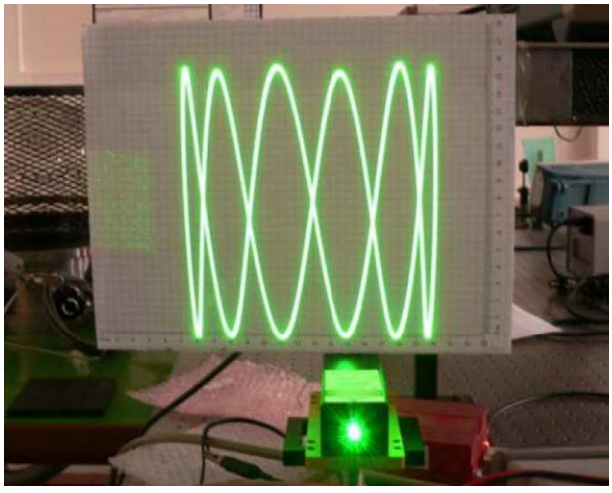

Fig. 8. 2D Lissajoux pattern created by the polymer scanner obtained by applying excitation signals at frequencies of 56.5 Hz and 340 Hz.

4. Fabrication

Fabrication of polymer-based scanners involved polymer moulding and permalloy electroplating. Polymer resin (Ren-Shape SL5195) is molded and cured by ultraviolet light into the desired scanner shape (Fig. 9(a)). The mould defines both the flexure and the mirror dimensions which are designed through FEM simulations. As illustrated in Fig. 1(a), the cantilever beam is anchored from the left and the rectangular plate on the right hand side supports the mirror and the magnetic material. In order

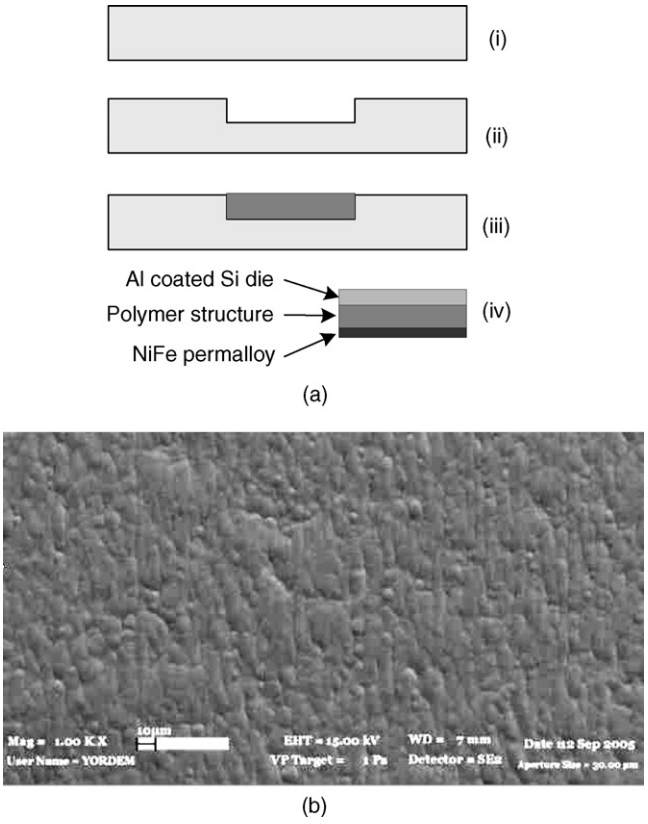

Fig. 9. (a) Fabrication sequence of the polymer scanner: (i) aluminum mould material; (ii) mould preperation for casting; (iii) polymer casting and UV curing of RenShape SL5195; (iv) release of structures and integration of Silicon mirror and NiFe permalloy. (b) SEM picture of the NiFe permalloy.

to minimize the distorting effects related to the deformation of the polymer scanner, Al coated silicon mirror die is integrated to the scanner using an insulating wax. In this fashion, silicon mirror is attached to the front side of the scanner and NiFe permalloy is deposited by electroplating on the back side, where the actuation force due to the magnetic field is exerted. NiFe layer electroplating is performed using a standard sulfate bath [11], at room temperature. Optimization of dc electroplating conditions with stress reducing agents resulted in thicknesses as much as 30 μm without running into residual stress problems. Scanning electron microscope photo of the plated NiFe permalloy is shown in Fig. 9(b).

5. Bar code reader application

Fig. 10 illustrates the block diagram of a barcode reader setup which utilizes an electromagnetic polymer scanner. Such a system can be partitioned into optical, mechanical and electrical blocks. Operation is based on creating a scan line on the barcode out of the light coming from the light source, then converting the reflected light into electrical signal by use of a photodiode and finally processing the signal using electronics.

The scanner explained in this paper is used in a barcode reader system as depicted in Fig. 10. A smaller coil than that was modeled in Section 2.2 is used to actuate the scanner and generate high in-plane and out-of-plane magnetic fields. The coil is driven

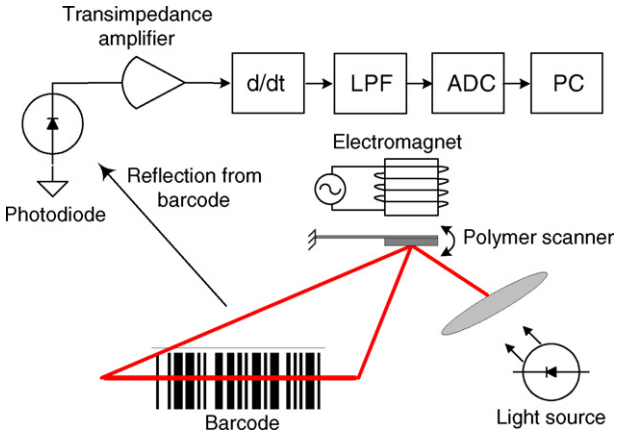

Fig. 10. Block diagram of a scanning mirror-based barcode reader system.

with a sinusoidal signal at the mechanical resonance of the scanner. Photograph of the prototype barcode reader setup is shown in Fig. 11(a), where light from a laser diode is incident on the scanner. The light is focused and scanned over the barcode. The scattered light is collected with a photo diode (PD) while the beam is scanned over the barcode. As illustrated in Fig. 11(b), PD output is a combination of peaks and valleys due to reflection from white and black stripes of the barcode.

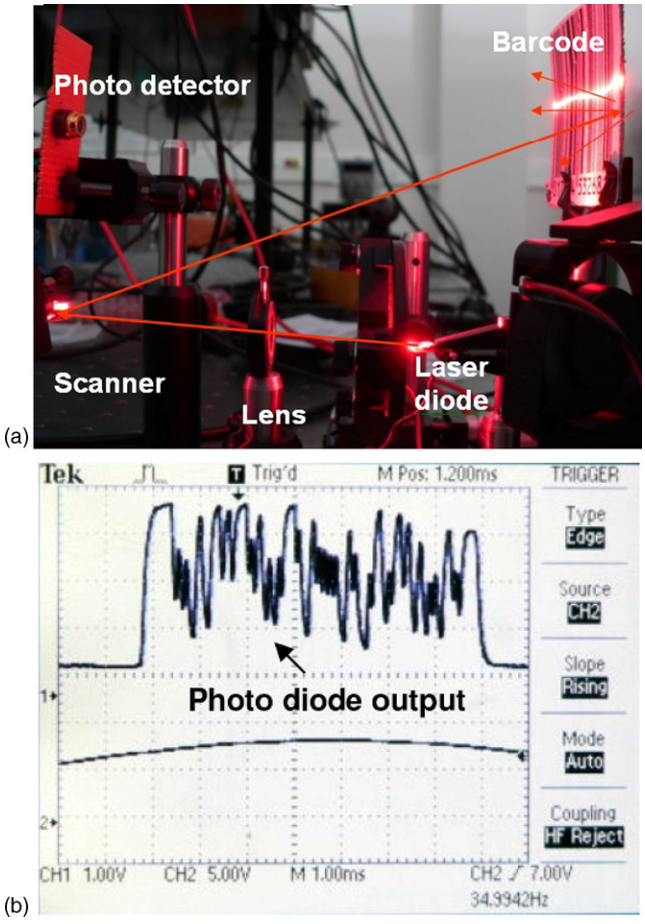

Fig. 11. (a) Photograph of the barcode scanner system during operation; (b) oscilloscope output of the photodiode.

The output of the photo diode is processed with an electronic circuitry to obtain the desired signal. As shown in Fig. 10, the current output of the photodiode is amplified and converted into voltage by a transimpedance amplifier. Time derivative of this amplified signal is taken to clearly find whether the scan line is crossing over a black or a white stripe on the barcode. Following that, analog to digital conversion with 10-bit resolution is performed to allow communication with a microcontroller used for decoding. Low resonance frequency of the scanner allows use of low-cost, widely available electronic components for data processing. Output of the photo diode on the scope is shown in Fig 11(b). The scope output is filtered then digitized and processed with the microprocessor. Different width black and white stripes in the original barcode are reconstructed using the distance between subsequent peaks in the scope signal. Different kinds of barcodes are scanned successfully by using this prototype setup.

6. Conclusions

An inexpensive, low resonant frequency polymer barcode scanner using magnetic permalloy actuator has been successfully developed. Very simple and low-cost fabrication processes using molded polymers and electroplated magnetic films for magnetic actuation have been developed. Unlike silicon-based micromachining, fabrication processes used in this work do not require clean room processing and photolithography [12,18,20,21]. It is shown that, the low resonance frequencies are easier to achieve with polymers due to low Young's modulus compared to Silicon MEMS scanners whose resonance frequency lies in the range of 1 kHz [19] to 22 kHz [12]. Low resoance frequency relieves the specifications of the electronics accompanying the scanner in barcode reading systems. Moreover, present design can achieve large total optical scan angle of 15.8° consuming a power of 168 mW (using a moderate electro coil drive voltage, 5 V for the specific coil used in this work), whereas silicon-based electrostatic scanners require rather high dc polarization (20–50 V) and ac excitation voltages (8–20 V) to get a comparable optical scan angle performance [14,15,17,19,20]. Most of the silicon-based magnetic scanners are surface micromachined [3–6] and therefore not suitable for mirror applications due to the dynamic deformation problem and low surface quality. Bulk micromachined silicon magnetic scanners suffers from both requirement of expensive fabrication steps such as deep reactive ion etching (DRIE), and relatively high frequencies for resonant mode operation [12,21].

Magnetic force is maximized by optimizing the placement of the scanner relative to the electro coil. One dimensional scanning at the fundamental resonance mode of the scanner is demonstrated. Resonant operation of the scanner allows filtering out the nonlinearities and hysteresis in the excitation torque, which is inherent in this type of magnetic actuator. The operation regime of small deflection angles has been studied and modeled. The prototype devices are tested using dynamic methods and the experimental results are shown to have good agreement with the theory. The scanning mirror is used in a barcode reading system. Scanners with smaller dimensions and similar structural materials can be utilized for better performance. The small angle operation of the device ensures low stress and therefore more reliable operation for the polymer.

Acknowledgements

Authors wish to thank Aselsan A.Ş., Ankara, Turkey for their help in fabrication of some of the prototypes. We are grateful to KUMPEM and Scientific and Technological Research Council of Turkey (TUBITAK) for funding of the project (grants MISAG-280-2004 and 104M161).

References

[1] G.F. Marshall (Ed.), Optical Scanning, Dekker, New York, 1991.
[2] O. Ergeneman, A.D. Yalcinkaya, H. Urey, Polymer based electromagnetic scanners for barcode applications, in: Proceedings of 16th Micromechanics Europe (MME) Workshop, 2005, pp. 370–373.
[3] B. Wagner, M. Kreutzer, W. Benecke, Electromagnetic microactuators with multiple degrees of freedom, in: Proceedings of the 6th International Conference on Solid State Sensors and Actuators (Transducers 1991), San Francisco, CA, USA, 1991, pp. 614–617.
[4] J. Judy, R.S. Muller, Magnetically actuated, addressable microstructures, IEEE J. Microelectromechan. Syst. 6 (3) (1997) 249–256.
[5] C. Liu, Micromachined magnetic actuators using electroplated permalloy, IEEE Trans. Magnetics 35 (3) (1999) 1976–1985.
[6] C. Liu, T. Tsao, G. Lee, J.T.S. Leu, Y.W. Yi, Y. Tai, C. Ho, Out-of-plane magnetic actuators with electroplated permalloy for fluid dynamics control, Sens. Acuators 78 (1999) 190–197.
[7] H. Urey, C. Kan, W. Davis, Vibration mode frequency formulae for micromechanical scanners, J. Micromech. Microeng. 15 (2005) 1713–1721.
[8] R.A. Miller, G.W. Burr, Y. Tai, D. Psaltis, Electromagnetic MEMS scanning mirrors for holographic data storage, in: Proceedings of the Solid State Sensor and Actuator Workshop, Hilton Head Island, 1996, pp. 183–186.
[9] S. Timoshenko, Strength of Materials, D. Van Nostrand Company, New Jersey, 1955.
[10] COMSOL FEMLAB version 3.1, Web page http://www.comsol.com.
[11] C.H. Ahn, M.G. Allen, A new toroidalmeander type integrated inductor with a multilevel meander magnetic core, IEEE Trans. Magnetics 30 (1, Parts 1–2) (1994) 73–79.
[12] A.D. Yalcinkaya, H. Urey, D. Brown, T. Montague, R. Sprague, Two-axis electromagnetic microscanner for high resolution displays, IEEE J. Microelectromechan. Syst. 15 (4) (2006) 786–794.
[13] Z. Yaqoob, A. Riza, Passive optics no-moving parts barcode scanners, IEEE Photonics Technol. Lett. 6 (3) (2004) 954–956.
[14] K. Meng-Hsiung, O. Solgaard, R.S. Muller, K. Lau, Micromachined polysilicon microscanners for barcode readers, IEEE Photonics Technol. Lett. 8 (12) (1996) 1707–1709.
[15] A. Wolter, H. Schenk, E. Gaumont, H. Lakner, MEMS microscanning mirror for barcode reading: from development to production, in: Proceedings of SPIE - MOEMS Display and Imaging Systems II, vol. 5348, 2004, pp. 32–39.
[16] R.S. Muller, K.Y. Lau, Surface-micromachined microoptical elements and systems, in: Proceedings of the IEEE (vol. 86, issue 8), 1998, pp. 1705–1720.
[17] A. Wolter, S.-T. Hsu, H. Schenk, H.K. Lakner, Applications and requirements for MEMS scanner mirrors, in: Proceedings of SPIE - MOEMS and Miniaturized Systems V (vol. 5719), 2005, pp. 64–75.
[18] E. Mounier, Y. de Charentenay, J.-C. Eloy, New applications for MOEMS, in: Proceedings of SPIE - MOEMS Display, Imaging, and Miniaturized Microsystems IV (vol. 114), 2006.
[19] J.-H. Lee, Y.-C. Ko, D.-H. Kong, J.-M. Kim, K.B. Lee, D.-Y. Jeon, Design and fabrication of scanning mirror for laser display, Sens. Actuators A 96 (2002) 223–230.

[20] H. Schenk, P. Durr, D. Kunze, H. Lakner, H. Kuck, A resonantly excited 2D-microscanning-mirror with large deflection, Sens. Actuators A 89 (2001) 104–111.
[21] H. Miyajima, Development of a MEMS electromagnetic optical scanner for a commercial laser scanning microscope, J. Microlithogr. Microfabric. Microsyst. 3 (2) (2004) 348–357.

Biographies

Arda D. Yalcinkaya received a BS degree from Istanbul Technical University, Electronics and Telecommunication Engineering Department, Istanbul, Turkey; MSc and PhD degrees from Technical University of Denmark (DTU), Mikroelektronik Centret, Kgs. Lynby, Denmark, all in electrical engineering in 1997, 1999 and 2003, respectively. Between 1999 and 2000 he was a research and development engineer at Aselsan Microelectronics, Ankara, Turkey. He had short stays as a visiting reseacher at Interuniversity Microelectronic Center (IMEC), Leuven, Belgium, Centro Nacionale de Microelectronica (CNM), Barcelona, Spain in 2000 and 2003. Since 2003, he has been a research associate at Koc University, Istanbul, where he is engaged with start up of a cleanroom facility. He is also working as a part time ASIC designer for Microvi-sion Inc., Seattle, USA. His research interests include design, fabrication and characterization of MEMS, CMOS-MEMS integration, nanotechnology and design of analog ASICs. He has been a Sabanci Foundation (VAKSA) scholar between 1992 and 1997, and a Turkish Education Foundation (TEV) scholar between 1997 and 1999.

Olgaç Ergeneman was born in Ankara, Turkey in 1981. He completed the high school in TED Ankara College in 1999. He received his BS degree from the Department of Electrical and Electronics Engineering, Middle East Technical University, Ankara in 2003. Same year, he joined Optical Microsystems Laboratory (OML) of Koc University, Department of Electrical Engineering as an MSc candidate. Olga Ergeneman is a student member of SPIE and IEEE.

Hakan Urey received the BS degree from Middle East Technical University, Ankara, Turkey in 1992, and MS and PhD degrees from Georgia Institute of Technology, Atlanta, Georgia, USA in 1996 and in 1997, all in electrical engineering. He is currently an assistant professor at Koc University, Istanbul, Turkey. He joined Microvision Inc., Seattle in 1998. Since 2002, he has been with Koc University. He has published more than 50 journals and conference papers, 5 edited books, 2 book chapters, and he has 9 issued and several pending patents. He is the chair of Photonics West MOEMS Display and Imaging Systems Conference and Photonics Europe Symposium MEMS, MOEMS, and Micromachining Conference. His research interests are generally in the area of information optics and microsystems, including microoptics, optical system design, microelectromechanical systems (MEMS), and display and imaging systems. Dr. Urey is a member of SPIE, OSA, IEEE-LEOS, and vice-president of the Turkey chapter of IEEE-LEOS.